**DOR: 20.1001.1.27170314.2023.12.1.6.9**

Research Paper

# Investigation of the Impact of the Alumina Powder Presence in Dielectric on Electrical Discharge Machining Parameters of A413 Aluminum Workpiece using Taguchi's Experiment Design, Signal-to-noise Analysis, and Total Normalized Quality Loss

**Mojtaba Shahbazi Dastjerdi[1], Ali Mokhtarian[1*], Mojtaba Rahimi[1]**
[1]Department of Mechanical, Civil, and Architectural Engineering, Khomeinishahr Branch, Islamic Azad University, Khomeinishahr/Isfahan, Iran
[*]Email of the Corresponding Author: mokhtarian@iaukhsh.ac.ir
*Received: February 4, 2023; Accepted: May 21, 2023*

**Abstract**

This study aimed to scrutinize the impact of the electrical discharge machining (EDM) parameters of A413 alloy for two cases of dielectric, one with alumina powder and one without, using Taguchi's experiment design method. The completed studies regarding the EDM of the metal-base composites reveal that insufficient research work has been carried out on this composite material. In this research, by using Taguchi's experiment design and through the simultaneous analysis of Total Normalized Quality Loss (TNQL) and Signal-to-Noise ratio (S/N) of the outputs, the impacts of the current intensity, voltage, pulse on-time, and pulse off-time on the material removal rate (MRR), surface roughness (SR), and tool wear rate (TWR) were investigated. The results showed that the use of 3g/L of alumina powder in kerosene dielectric averagely led to a 6.47%, 9.14%, and 19.40% reduction in MRR, SR, and TWR, respectively. Also, the results acquired using TNQL and S/N analyses demonstrated that the optimum experiment was composed of the third level of voltage (A3), the first level of current (B1), the first level of pulse on-time (C1), and the third level of pulse-off time (D3). It was concluded that the current intensity had the greatest impact on the MRR and SR. However, the pulse-on time had the greatest influence on the TWR. It was also observed that the MRR declined by adding 3g/L aluminum oxide powder in the kerosene dielectric which in turn caused a reduction in the SR and the TWR compared to the case of the kerosene dielectric without powder.

**Keywords**

Electrical Discharge Machining, A413 Aluminum, Alumina Powder, Signal-to-Noise Ratio, Total Normalized Quality Loss

**Abbreviation**

| | |
|---|---|
| EDM: electrical discharge machining | ANOVA: analysis of variance |
| TNQL: Total Normalized Quality Loss | MSNR: Multi-Signal-to-Noise Ratio |
| S/N: Signal-to-Noise ratio | MRR: material removal rate |
| TWR: tool wear rate | SR: surface roughness |
| DF: Degrees of Freedom | SS: Sum of Squares |
| MS: Mean of Squares | |

## 1. Introduction

Electrical discharge machining (EDM) can machine a broad range of conductive materials. In this method, two metal electrodes, one with a predetermined shape and the other a workpiece, are submerged in a dielectric liquid. With the collision of ions and electrons with the workpiece and tool, a very high temperature will create, which causes the superheated metal to evaporate and the material removal operation to occur as a result [1]. Given the very high costs of this type of machining and the need for a reduction in the final cost of these products, various investigations have been conducted to adjust the optimum machining parameters of the EDM [2]. The surface analysis method in the investigation of the effect of input parameters of current, voltage, pulse on-time, and pulse off-time on the material removal rate (MRR), tool wear rate (TWR), and composite surface roughness (SR) of aluminum 7075 indicated that the MRR increased with the increase of pulse on-time initially, however, it decreased with further increase in pulse on-time ultimately [3]. The results of the investigation on the EDM parameters of Nickel C1023-base alloy showed that current and pulse time was the most influencing parameters. For having the least tool wear, a small pulse on-time and current intensity should be chosen. Also, for high current intensity, the best result was obtained when the pulse on time was large, and for low current intensity, the best outcome was achieved when the pulse on time was small [4]. The analysis results of gap variations, plasma channel changes, and plasma electromagnetic variations in the EDM indicated that the oscillation of the plasma discharge in the EDM was a mixed process that was activated by various factors. These factors included the electrical region of the gap, the conductivity of the plasma channel, dielectric pressure, and gap geometry. Note also that the role of fluctuating pulses, which were active in the enhancement of the EDM efficiency, was very significant [5]. In the milling process on AISI 304 stainless steel using the EDM method, the influences of air-blowing rate, voltage, and electrode rotation speed on the MRR and SR were examined. The outcomes suggested that the MRR increased with the increase of air blowing, current, voltage, and tool rotation speed. On top of that, a decrease in current resulted in a reduction in the SR [6]. The results of the use of Taguchi's experiment design in the examination of effective parameters of the EDM of AZ31 magnesium alloy revealed that the pulse on-time parameter was the most important influential parameter on the SR compared to other parameters (i.e., voltage, current intensity, and pulse off-time) [7]. In another research, the SR was examined during the EDM of AISI 4340 steel using a tungsten copper electrode. The residual stress due to the EDM was measured by using the X-Ray method. The research outcomes indicated that the MRR and SR increased with the increase of the current intensity generally. Furthermore, the increase in the current intensity gave rise to an increase in the growth of the cracks [8]. To minimize the TWR and increase the MRR of the Nanocomposite Aluminum-Boron Carbide, increasing the pulse on time for all states of the highest current was very effective [9]. To reach the maximum MRR in the alloy DIN 1.2080, the two parameters of current and pulse on-time were set at their top level and the pulse off-time at the minimum level. Because of this, the maximum discharge energy was created and a favorable MRR was achieved. The voltage parameter had the most minor impact on MRR changes [10]. Considering the use of CK45 in the manufacturing of forging molds and the need for suitable SR, two parameters of the current and the pulse on time were controlled with considerable sensitivity during the EDM process of this steel [11]. In the EDM of HARDOX-400 steel, the increase of the ratio of pulse on-time to pulse off-time reduced MRR. Furthermore, the increase of the current along with the increase of the pulse on time led to an increase in the SR of the workpiece [12]. Applying vibration to the workpiece causes the MRR and SR to substantially improve. In the EDM of the SKD61 workpiece, by applying vibration to the workpiece, it was observed that low-frequency vibration can increase MRR and control spark energy. Moreover, low-frequency vibration significantly improved the machined surface [13]. The performed studies in the EDM of the metal-based composites reveal that inadequate investigations have been carried out on this composite material. To fill this research gap, the impact of alumina powder presence within the dielectric on output parameters of the MRR, SR, and TWR was scrutinized during the EDM of A413 aluminum through Taguchi's experiment design. Moreover, after performing the analysis of variance (ANOVA), the effect of the input parameters of voltage, current intensity, pulse on time, and pulse off-time was investigated by the novel approach of using the simultaneous analysis of Total Normalized Quality Loss (TNQL) and Signal-to-Noise ratio (S/N) of the outputs for two cases of dielectric with and without alumina powder.

## 2. Materials and Equipment

The materials used in this study included the workpiece of aluminum alloy, machining tools or copper electrodes, and dielectric. The A413 alloy workpiece has very extensive applications. It is employed in high-pressure situations, for example in sensitive hydraulic cylinders, pressure valves and containers, and so on. Also, because of its outstanding heat treatment and abrasion resistance, this alloy is a remarkable choice for use in abrasive applications [14]. The percentage of elements and some of the physical and mechanical properties of this alloy are exhibited in Table 1 [15].

Table 1. Physical and mechanical properties of 413 aluminum [15]

**Detailed Composition**

| Si | Fe | Cu | Mg | Mn | Ni | Zn | Sn | Ti | Others | Total | Al |
|---|---|---|---|---|---|---|---|---|---|---|---|
| 11.0-13.0 | 1.3 | 1.0 | 0.10 | 0.35 | 0.50 | 0.50 | 0.15 | - | - | 0.25 | Balance |

**Mechanical Properties**

| Ultimate Tensile Strength (MPa) | Yield Strength (MPa) | Elongation (% in 51 mm) | Hardness (BHN) | Shear Strength (MPa) | Fatigue Strength (MPa) |
|---|---|---|---|---|---|
| 290 | 130 | 3.5 | 80 | 170 | 130 |

**Physical Properties**

| Density ($g/cm^3$) | Melting Range (˚c) | Specific Heat (J/kg ˚c) | Coefficient of Thermal Expansion (µm/m˚k) | Thermal Conductivity (W/m˚k) | Electrical Conductivity (%IACS) |
|---|---|---|---|---|---|
| 2.66 | 574-582 | 963 | 21.6 | 121 | 31 |

The electrode employed in this research was made of pure copper (99.9%) with a diameter of 10 mm and a height of 150 mm. Besides, two types of kerosene dielectric and kerosene dielectric mixed with alumina powder were utilized. For the case of the dielectric mixed with alumina powder, 3 g/L of alumina powder was added to kerosene according to the designed experiment. Moreover, the spark machine manufactured by the Tehran-Ekram company was used to conduct the experiments. To measure the MRR and TWR, a laboratory-accurate scale (AND GR-300 model) with a precision of 0.001 g was employed. The masses of the electrode (tool) and workpiece were measured before and after machining using this scale. At the end of the machining operation, the $R_a$ values of machined areas of workpieces (surface of workpiece bottom) were measured through a roughness meter apparatus (Mahr M300-RD18 model) with a precision of one micrometer.

## 3. Experiment design

Four parameters of voltage, current intensity, pulse on time, and pulse off-time were considered as input parameters. Given the adjustable parameters of the spark machine (Tehran-Ekram model), two levels for voltage and three levels for other parameters were considered (Table 2). By applying Taguchi's experiment design method, the impacts of input parameters of the EDM on the MRR, the workpiece SR, and TWR were examined by using Minitab@17 software for two cases with and without the presence of alumina powder in kerosene dielectric. Because of the existence of four factors (i.e., input parameters) and also the selection of three levels for each factor, Taguchi's method with an L9 orthogonal array was selected (Table 3). The duration of each experiment was chosen to be five minutes. Furthermore, the components of the experiments were washed completely with acetone in each step of the experiments. Then after drying, the masses of the electrode and workpiece were measured using the above-mentioned scale. To be sure about the accuracy of the adjustment parameters on the sparking apparatus, an oscilloscope was utilized to accurately adjust the pulse on time and pulse off-time. Moreover, a multimeter apparatus was employed to check the voltage and current of the spark apparatus. Ultimately, the roughness of the machined surfaces of the workpiece was measured by the roughness meter apparatus.

Table 2. Regulatory parameters of the apparatus in each step of the experiments

| Factors | Regulatory levels | | |
|---|---|---|---|
| Related levels of Taguchi's method | 1 | 2 | 3 |
| Voltage (V) | 80 | 250 | 80 |
| Current (A) | 10 | 15 | 20 |
| Pulse On-Time (μses) | 35 | 50 | 100 |
| Pulse Off-Time (μsec) | 30 | 70 | 200 |

Table 3. The parameters of Taguchi's experiments

| Experiment No. | Voltage | Current Intensity | Pulse On-Time | Pulse Off-Time |
|---|---|---|---|---|
| 1 | 1 | 1 | 1 | 1 |
| 2 | 1 | 2 | 2 | 2 |
| 1 | 1 | 3 | 3 | 3 |
| 4 | 2 | 1 | 2 | 3 |
| 5 | 2 | 2 | 3 | 1 |
| 6 | 2 | 3 | 1 | 2 |
| 7 | 1 | 1 | 3 | 2 |
| 8 | 1 | 2 | 1 | 3 |
| 9 | 1 | 3 | 2 | 1 |

The volumetric MRR was calculated in cubic millimeters per minute ($mm^3$/min) using Equation (1) as follows:

$$MRR = \frac{(W_1 - W_2)}{\rho_w \times t} \times 10^3 \quad (1)$$

where $W_1$ and $W_2$ are the weight of the workpiece before and after machining, $\rho_w$ is the density of the workpiece, and $t$ is the machining time in minutes.

The TWR was computed in cubic millimeters per minute ($mm^3$/min) according to Equation (2) as follows:

$$TWR = \frac{(T_1 - T_2)}{\rho_T \times t} \times 10^3 \quad (2)$$

where $T_1$ and $T_2$ are the tool weight before and after machining, $\rho_T$ is the electrode density, and $t$ is the machining time in minutes.

The values of the MRR, SR, and TWR obtained from the experiments are presented in Table 4.

To perform the S/N analysis, the MRR values were calculated using Equation 3 (the larger, the better). Moreover, the SR and TWR were computed using Equation 4 (the smaller, the better).

$$S/N = -10 \log(\frac{1}{n}\sum_{i=1}^{n}\frac{1}{y_i^2}) \quad (3)$$

$$S/N = -10 \log(\frac{1}{n}\sum_{i=1}^{n} y_i^2) \quad (4)$$

In Equations (3-4), $n$ is the number of tests and $y_i$ are the measured values.

Table 4. The results of experiments conducted on 413 aluminum workpieces in two cases with and without alumina powder

| Experiment No. | Kerosene dielectric (Experiment No. 1) | | | Kerosene dielectric containing 3 g/L of alumina powder (Experiment No.2) | | |
|---|---|---|---|---|---|---|
| | **MRR** | **SR** | **TWR** | **MRR** | **SR** | **TWR** |
| 1 | 2.1834 | 5.379 | 0.0383 | 1.8755 | 4.674 | 0.0296 |
| 2 | 2.9518 | 9.391 | 0.0414 | 2.2651 | 8.682 | 0.0329 |
| 3 | 3.4061 | 12.144 | 0.0329 | 3.093 | 11.457 | 0.0285 |
| 4 | 2.2817 | 5.011 | 0.042 | 2.2565 | 3.508 | 0.0332 |
| 5 | 5.7246 | 9.051 | 0.0327 | 5.4232 | 8.340 | 0.0271 |
| 6 | 3.3842 | 8.544 | 0.0439 | 3.0846 | 7.851 | 0.0350 |
| 7 | 2.5687 | 5.640 | 0.0309 | 2.1628 | 4.619 | 0.0260 |
| 8 | 1.4764 | 9.219 | 0.041 | 1.1725 | 8.517 | 0.0322 |
| 9 | 5.6702 | 12.146 | 0.0412 | 5.9714 | 11.883 | 0.0330 |

Because the MRR, SR, and TWR had different units, they had to become dimensionless to enable us to perform simultaneous optimization. In this regard, to carry out the normalization operation, the data related to each output should be divided by the maximum value of that output. Then for the simultaneous calculation of TNQL and S/N ratio, the outputs were given a weight based on their importance (Equation 5). Also, the cumulative normalized value of parameters was computed using Equation 6. Because of the higher importance of the MRR compared to the SR and TWR, the weight ratio value of the MRR, SR, and TWR was considered to be 0.5, 0.3, and 0.2, respectively.

$$TNQLi = \sum Wy = (0.5\, MRR + 0.3\, Ra + 0.2\, TWR) \quad (5)$$

$$MSNRi = -10\, Log\, (TNQLi) \quad (6)$$

After the calculation of the average value of MSNR (i.e. Multi-Signal-to-Noise Ratio) for each parameter in different levels, the average value of MSNR was calculated for each input parameter and its various levels using Equation 7 according to Taguchi's method and MSNR values.

$$\eta_0 = \eta m + \sum (\eta i - \eta m) \quad (7)$$

where $\eta i$ and $\eta m$ are the S/N ratio for each step and the average S/N ratio for all steps, respectively. Finally, the maximum value procured for each input parameter was considered the optimum value [17].

## 4. Results and discussion

*4.1 Analysis of the MRR Results*

According to the diagram of Figure 1, the current intensity and pulse off-time had the largest slope on their curves and hence, they had the largest influence. With the increase in the current intensity, the temperature of the workpiece surface increased under the increase in the spark energy. This increased melting and hence, the evaporation of the workpiece surface and MRR increased rapidly. With the increase of the current intensity and pulse on time, the number of cations colliding with the workpiece surface increased. Therefore, the two diagrams showed an upward trend. However, due to the accumulation of the workpiece swarfs in the machining area, the energy density diminished in the electrical discharge area. This caused the gradient of the material removal slope to reduce.

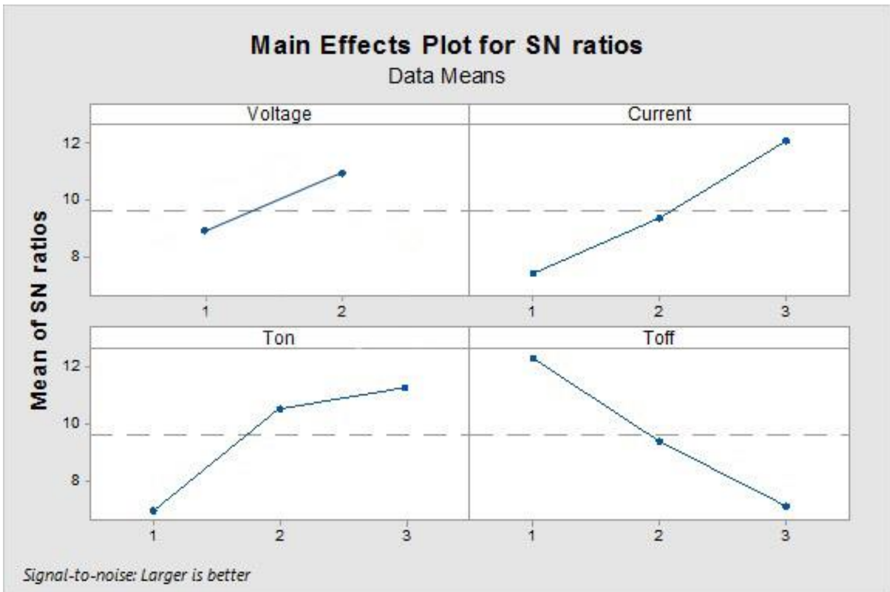


Figure 1. The effects of the machining input parameters of the first experiment on the MRR

The MRR of the workpiece in the case of the machining in kerosene dielectric with 3 g/L of alumina powder was less than the kerosene dielectric without alumina powder (Figure 2). The reason was that the existence of alumina powder in the dielectric decreased the spark energy, causing a reduction in the MRR.

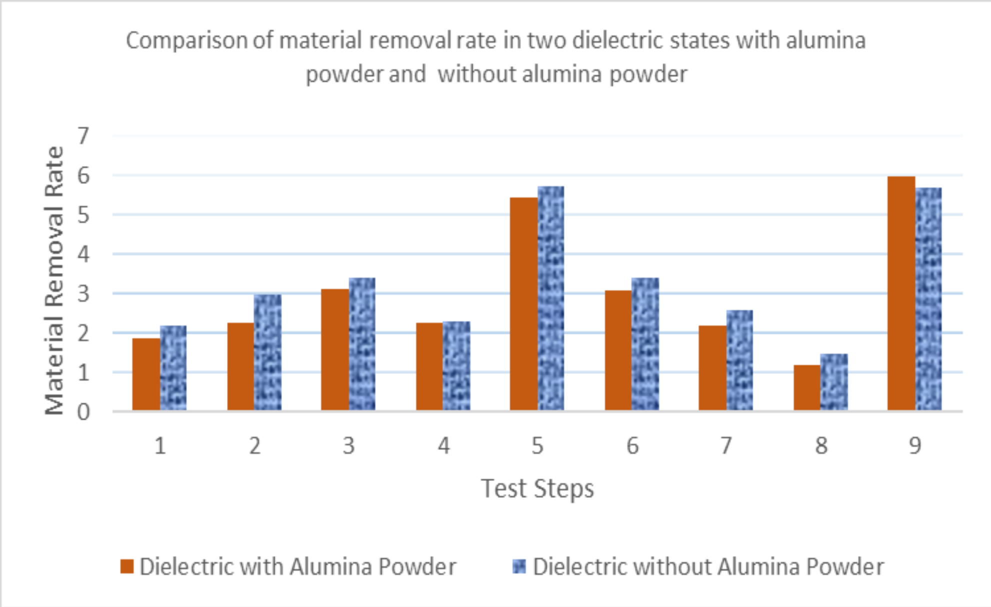


Figure 2. Comparison of the MRR in two experiments with and without alumina powder

Tables of the variance analysis (Tables 5-6) indicated that for a confidence level of 95% with a p-value smaller than 0.05, the effects of pulse off-time, current intensity, pulse on-time, and voltage for the first experiment, and the impacts of pulse off-time, pulse on-time, current intensity, and voltage for the second experiment were respectively the most crucial.

Table 5. The results of the variance analysis of the MRR in the first experiment

| Parameter | Degrees of Freedom (DF) | Sum of Squares (SS) | Mean of Squares (MS) | F-Value | P-Value | Degree of Impact (Rank) |
|---|---|---|---|---|---|---|
| Voltage | 1 | 1.1370 | 1.1370 | 4.7821 | 0.06498 | 4 |
| Current | 2 | 4.9448 | 2.4724 | 11.5586 | 0.00875 | 2 |
| Pulse On-Time | 2 | 4.1338 | 2.0669 | 9.0881 | 0.01528 | 3 |
| Pulse Off-Time | 2 | 3.6673 | 3.6673 | 21.0652 | 0.001937 | 1 |

Table 6. The results of the variance analysis of the MRR in the second experiment

| Parameter | Degrees of Freedom (DF) | Sum of Squares (SS) | Mean of Squares (MS) | F-Value | P-Value | Degree of Impact (Rank) |
|---|---|---|---|---|---|---|
| Voltage | 1 | 1.1573 | 1.1573 | 4.1632 | 0.08066 | 4 |
| Current | 2 | 3.5891 | 1.7945 | 6.3237 | 0.03331 | 3 |
| Pulse On-Time | 2 | 4.8461 | 2.4230 | 9.2192 | 0.014799 | 2 |
| Pulse Off-Time | 2 | 8.4388 | 4.2194 | 20.7958 | 0.002004 | 1 |

### *4.2 Analysis of the SR Results*

According to Figure 3, the current intensity had the largest slope and hence, the highest impact. With the augmentation of the current intensity and pulse on time, the surface roughness increased. This was because, with more intense activation of cations, the spark energy increased. This resulted in a heavier bombardment of the ions on the workpiece, causing more holes on the workpiece surface.

Besides, with the increase in pulse on time, the current density and input thermal flux to the surface lessened because of the high extension of the plasma channel. Hence, the depth of the created holes diminished and thus, the SR of the workpiece decreased.

Figure 4 exhibits that due to the high electrical resistivity of alumina powder, the spark was distributed on the surface of the workpiece with less intensity. These factors slightly raised the SR of the workpiece in the case of machining in a dielectric without alumina powder compared to the case with alumina powder.

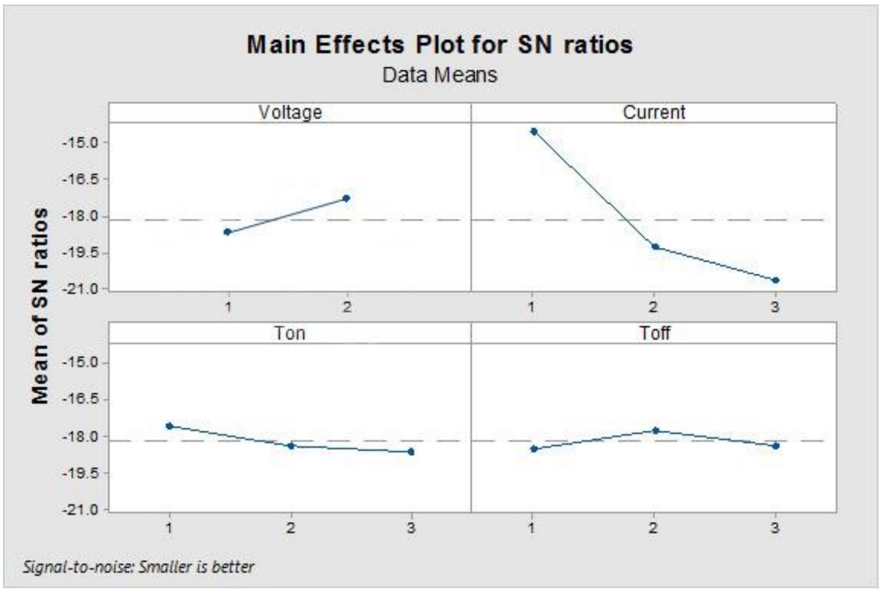


Figure 3. The effects of the machining input parameters of the first experiment on the SR

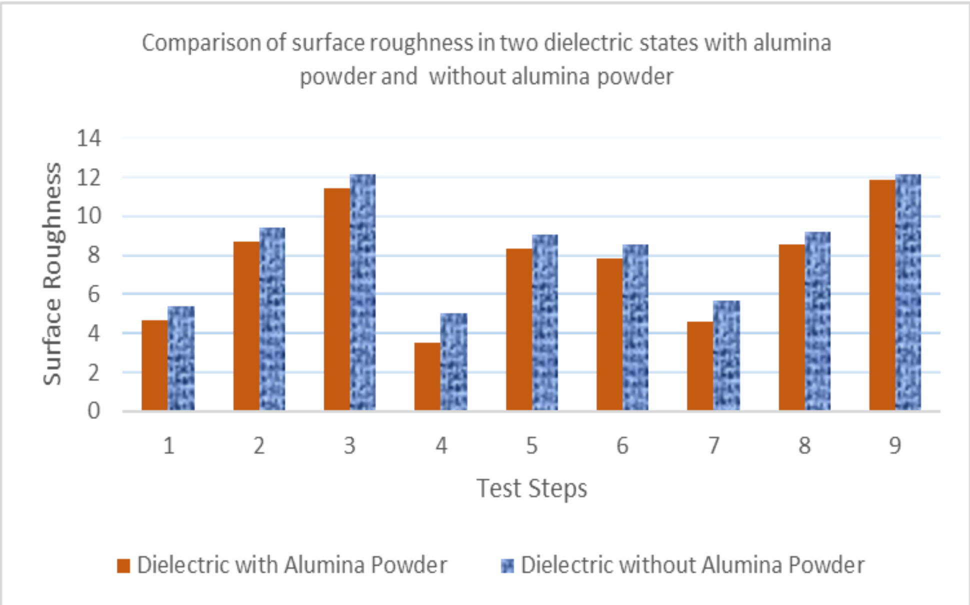


Figure 4. Comparison of the SR in two experiments with and without alumina powder

Tables of the variance analysis (Tables 7 and 8) demonstrated that the impacts of current intensity, voltage, pulse on-time, and pulse off-time for the first experiment, and the influences of current intensity, voltage, pulse off-time, and pulse on-time for the second experiment were respectively the most important effects.

Table 7. The results of the variance analysis of the SR in the first experiment

| Parameter | Degrees of Freedom (DF) | Sum of Squares (SS) | Mean of Squares (MS) | F-Value | P-Value | Degree of Impact (Rank) |
|---|---|---|---|---|---|---|
| Voltage | 1 | 13.3143 | 13.3143 | 17.2362 | 0.00428 | 2 |
| Current | 2 | 58.4827 | 29.2413 | 19.7110 | 0.002305 | 1 |
| Pulse On-Time | 2 | 11.9157 | 5.9579 | 6.4447 | 0.03204 | 3 |
| Pulse Off-Time | 2 | 10.9781 | 5.4891 | 5.8381 | 0.03911 | 4 |

Table 8. The results of the variance analysis of the SR in the second experiment

| Parameter | Degrees of Freedom (DF) | Sum of Squares (SS) | Mean of Squares (MS) | F-Value | P-Value | Degree of Impact (Rank) |
|---|---|---|---|---|---|---|
| Voltage | 1 | 6.0482 | 6.0482 | 6.6317 | 0.03672 | 2 |
| Current | 2 | 59.1549 | 29.5774 | 16.5267 | 0.003627 | 1 |
| Pulse On-Time | 2 | 2.2987 | 1.1494 | 1.0204 | 0.41548 | 4 |
| Pulse Off-Time | 2 | 2.3839 | 1.1919 | 1.0593 | 0.40365 | 3 |

*4.3 Analysis of the TWR Results*

As shown in Figure 5, the diagram of the pulse on-time parameter had the greatest impact. Because the workpiece had a negative charge and the electrode had a positive charge, the plasma channel diameter increased as the pulse on time increased. Furthermore, the attack of electrons toward the electrode was overcome by the attack of cations on the workpiece surface. Therefore, with the increase of pulse on-time up to 50 $\mu sec$, the TWR raised slightly and then decreased quickly.

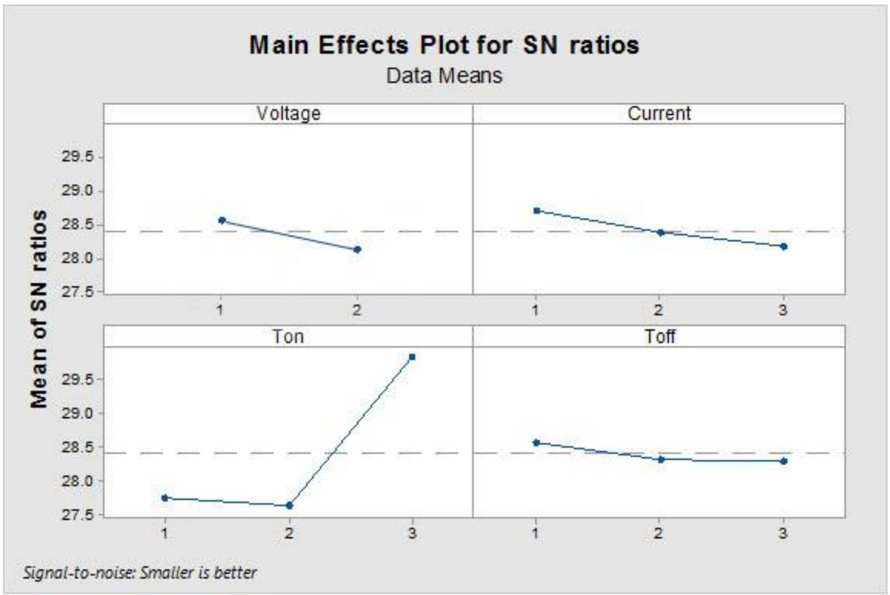


Figure 5. The effects of the machining input parameters of the first experiment on the TWR

As for the machining with dielectric containing alumina powder, the TWR decreased under the decrease in the spark energy (Figure 6).

Tables of the variance analysis (Tables 9-10) revealed that for a confidence level of 95% with a p-value smaller than 0.05, the effects of pulse on-time, current intensity, voltage, and pulse off-time were the most crucial and critical effects for both experiments, respectively.

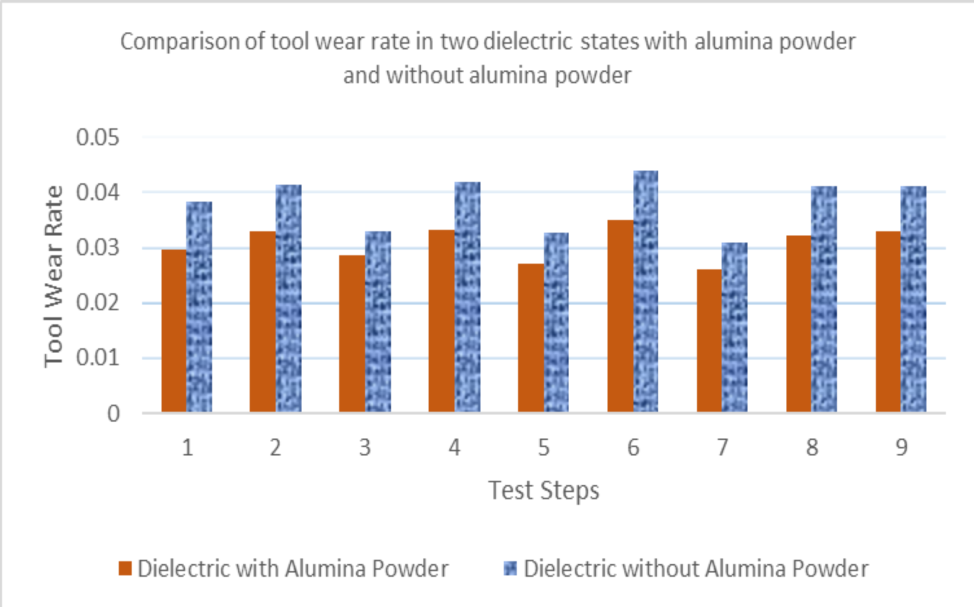


Figure 6. Comparison of the TWR in two experiments with and without alumina powder

Table 9. The results of the variance analysis of the TWR in the first experiment

| Parameter | Degrees of Freedom (DF) | Sum of Squares (SS) | Mean of Squares (MS) | F-Value | P-Value | Degree of Impact (Rank) |
|---|---|---|---|---|---|---|
| Voltage | 1 | 0.000726 | 0.000726 | 38.9694 | 0.00427 | 3 |
| Current | 2 | 0.000735 | 0.0003675 | 19.6629 | 0.00232 | 2 |
| Pulse On-Time | 2 | 0.016587 | 0.0082935 | 33.7801 | 0.000543 | 1 |
| Pulse Off-Time | 2 | 0.000318 | 0.0000159 | 6.2012 | 0.03466 | 4 |

Table 10. The results of the variance analysis of the TWR in the second experiment

| Parameter | Degrees of Freedom (DF) | Sum of Squares (SS) | Mean of Squares (MS) | F-Value | P-Value | Degree of Impact (Rank) |
|---|---|---|---|---|---|---|
| Voltage | 1 | 0.000396 | 0.000396 | 73.3332 | 0.006862 | 3 |
| Current | 2 | 0.001023 | 0.0005115 | 12.7875 | 0.000594 | 2 |
| Pulse On-Time | 2 | 0.006015 | 0.0030075 | 34.4738 | 0.000513 | 1 |
| Pulse Off-Time | 2 | 0.000393 | 0.0001965 | 3.0417 | 0.122431 | 4 |

*4.4 Simultaneous analysis of the output S/N ratios of the EDM process*

In this section, using the simultaneous analysis of TNQL and S/N ratios of the outputs, the impacts of the parameters of current intensity, voltage, pulse on-time, and pulse off-time on the MRR, SR, and TWR were investigated for the two cases of dielectric with and without alumina powder.

- 413 Aluminum in kerosene dielectric

The results of the S/N ratio analysis and normalized outputs are presented in Table 11. The maximum values of the S/N ratio are grayed in the table.

Table 11. Results of S/N ratio analysis and normalized outputs of the first experiment

| Experiment No. | S/N ratio analysis | | | Normalized outputs | | |
|---|---|---|---|---|---|---|
| | **MRR** | **SR** | **TWR** | **MRR** | **SR** | **TWR** |
| 1 | 6.7826 | 14.6140 | 28.3360 | 0..4475 | 0.6738 | 0.9382 |
| 2 | 9.4017 | 19.4542 | 27.6599 | 0.6203 | 0.8969 | 0.9158 |
| 3 | 10.6451 | 21.6872 | 29.6560 | 0.7024 | 0.9999 | 0.9819 |
| 4 | 7.1651 | 13.9984 | 27.5350 | 0.4727 | 0.6454 | 0.9117 |
| 5 | 15.1549 | 19.1339 | 29.7090 | 1 | 0.8822 | 0.9837 |
| 6 | 10.5891 | 18.6332 | 27.1507 | 0.6987 | 0.8591 | 0.8990 |
| 7 | 8.1942 | 15.0255 | 30.2008 | 0.5406 | 0.6927 | 1 |
| 8 | 3.3840 | 19.2936 | 27.7443 | 0.2232 | 0.8895 | 0.9186 |
| 9 | 15.0719 | 21.6886 | 27.7020 | 0.9945 | 1 | 0.9172 |

The outcomes of the normalization and the simultaneous analysis of the S/N ratios of the outputs are presented in Table 12. Note that for the MRR, SR, and TWR, the weight ratio of 0.5, 0.3, and 0.2 was allocated, respectively.

Table 12. Results of normalization and simultaneous analysis of S/N ratios of the outputs of the first experiment

| Experiment No. | TNQL | MSNR |
|---|---|---|
| 1 | 0.61353 | 2.12164 |
| 2 | 0.76238 | 1.17828 |
| 3 | 0.84755 | 0.71834 |
| 4 | 0.61231 | 2.13028 |
| 5 | 0.9614 | 0.17095 |
| 6 | 0.78688 | 1.04091 |
| 7 | 0.67811 | 1.68699 |
| 8 | 0.56217 | 2.50132 |
| 9 | 0.98069 | 0.08468 |
| MSNR average | | 1.29259 |

According to the average MSNR for each input parameter in different levels (Table 13), the ultimate result of the analysis indicated the third level of voltage ($A_3$), the first level of current intensity ($B_1$), the first level of pulse on time ($C_1$), and the third level of pulse off-time ($D_3$).

Table 13. Average MSNR for each input parameter in different levels for the first experiment

| Input parameters | Average MSNR for each input parameter in different levels | | |
|---|---|---|---|
| | Level 1 | Level 2 | Level 3 |
| Voltage (A) | 1.43308 | 0.75696 | 1.68781 |
| Current (B) | 2.70765 | 1.26537 | 0.74125 |
| Pulse on-time (C) | 3.07869 | 0.80806 | 0.0089 |
| Pulse off-time (D) | 0.20791 | 1.321 | 2.76476 |

- 413 aluminum in kerosene dielectric containing 3 g/L of alumina powder

The results of the S/N ratio analysis and normalized outputs are presented in Table 14. The maximum values of the S/N ratio are grayed in the table.

Table 14. Results of S/N ratio analysis and normalized outputs of the second experiment

| Experiment No. | S/N ratio analysis | | | Normalized outputs | | |
|---|---|---|---|---|---|---|
| | **MRR** | **SR** | **TWR** | **MRR** | **SR** | **TWR** |
| 1 | 5.4623 | 13.3937 | 30.5741 | 0.3519 | 0.6230 | 0.9644 |
| 2 | 8.5792 | 18.7723 | 29.6560 | 0.5527 | 0.8731 | 0.9355 |
| 3 | 9.8196 | 21.1814 | 30.9031 | 0.6326 | 0.9852 | 0.9748 |
| 4 | 7.0687 | 10.9011 | 29.5772 | 0.4554 | 0.5070 | 0.9330 |
| 5 | 14.6851 | 18.4233 | 31.3406 | 0.9461 | 0.8569 | 0.9886 |
| 6 | 9.7839 | 17.8984 | 29.1186 | 0.6303 | 0.8325 | 0.9185 |
| 7 | 6.7003 | 13.2909 | 31.7005 | 0.4316 | 0.6182 | 1 |
| 8 | 1.3822 | 18.6057 | 29.8428 | 0.0890 | 0.8645 | 0.9413 |
| 9 | 15.5215 | 21.4985 | 29.6297 | 1 | 1 | 0.9346 |

The normalization results and S/N ratio simultaneous analysis of the outputs are presented in Table 15. For the MRR, SR, and TWR, a weight ratio of 0.5, 0.3, and 0.2 was assigned, respectively. According to the average MSNR for each input parameter in different levels (Table 16), the final result of the analysis suggested the third level of voltage ($A_3$), the first level of current intensity ($B_1$), the first level of pulse on time ($C_1$), and the third level of pulse off-time ($D_3$).

Table 15. Results of normalization and simultaneous analysis of S/N ratios of the outputs of the second experiment

| Experiment No. | TNQL | MSNR |
|---|---|---|
| 1 | 0.55573 | 2.55136 |
| 2 | 0.72538 | 1.39434 |
| 3 | 0.80682 | 0.93223 |
| 4 | 0.5664 | 2.56876 |
| 5 | 0.92784 | 0.32526 |
| 6 | 0.74680 | 1.25750 |
| 7 | 0.60126 | 2.20937 |
| 8 | 0.49238 | 3.07699 |
| 9 | 0.98692 | 0.05718 |
| MSNR average | | 1.58588 |

Table 16. Average MSNR for each input parameter in different levels for the second experiment

| Input parameters | Average MSNR for each input parameter in different levels | | |
|---|---|---|---|
| | Level 1 | Level 2 | Level 3 |
| Voltage (A) | 1.70625 | 0.87984 | 2.17178 |
| Current (B) | 4.05773 | 1.62483 | 0.92458 |
| Pulse on-time (C) | 3.71409 | 0.74852 | 0.2951 |
| Pulse off-time (D) | 0.23796 | 1.68945 | 3.30622 |

## 5. Conclusion

The objective of this study was to scrutinize the effect of the presence of alumina powder in kerosene dielectric on the EDM parameters of A413 aluminum through Taguchi's experiment design and the analyses of the S/N ratio and TNQL. It was concluded that the current intensity and pulse off-time had the greatest impact on the MRR. With the rise of the pulse on time and voltage, the MRR increased. However, it decreased with the increase of pulse off-time. Moreover, the current intensity parameter was the most influencing parameter on the SR. Following the increase in the current intensity, the SR increased rapidly, and after a rise in voltage and pulse off-time, the SR diminished. With the increase in pulse off-time (more than 70 $\mu sec$), the SR increased gently again. Furthermore, following the increase in pulse on-time up to 50 $\mu sec$, the SR increased initially and then decreased thereafter. Among the influential input parameters on the TWR, pulse on time had the greatest impact. After the elevation of voltage and current intensity, the TWR increased. Besides, with the rise of pulse on-time after 50 $\mu sec$, the TWR lessened promptly. It was found that the addition of 3 g/L of alumina powder to kerosene dielectric in the EDM of A413 aluminum not only decreased the MRR but also diminished the SR and TWR as well.

## 6. References

[1] Hourmand, M., Farahany, S., Sarhan, A., and Noordin, M. 2015. Investigating the electrical discharge machining (EDM) parameter effects on Al-Mg2Si metal matrix composite (MMC) for high material removal rate (MRR) and less EWR–RSM approach. The International Journal of Advanced Manufacturing Technology. 77(8): 831-838.

[2] Satpathy, A., Tripathy, S., Senapati, N. and Brahma, M. 2017. Optimization of EDM process parameters for AlSiC-20% SiC reinforced metal matrix composite with multi-response using TOPSIS. Materials Today: Proceedings. 4(2): 3043-3052.

[3] Gopalakannan, S., Senthilvelan, T. and Ranganathan, S. 2012. Modeling and Optimization of EDM Process Parameters on Machining of Al 7075-B4C MMC Using RSM. Procedia Engineering. 38: 685-690.

[4] Ayesta, I. 2013. Influence of EDM Parameters on Slot Machining in C1023 Aeronautical Alloy. Procedia CIRP. 6: 129-134.

[5] Wei, D., Di, S., Wang, Y. and Wang, Z. 2016. Analyzing of Discharge Wave Oscillation Mechanism in Electrical Discharge Machining. Procedia CIRP. 42: 23-27.

[6] Shen, Y., Liu, Y. and Sun, W. 2016. High-efficient Dry Hybrid Machining of EDM and Arc Machining. Procedia CIRP. 42: 149-154.

[7] Razak, M., Abdul-Rani, A., Rao, T., Pedapati, S. and Kamal, S. 2016. Electrical Discharge Machining on Biodegradable AZ31 Magnesium Alloy Using Taguchi Method. Procedia Engineering. 148: 916-922.

[8] Rizvi, S., and Agarwal, S. 2016. An Investigation on surface integrity in EDM Process with a Copper Tungsten Electrode. Procedia CIRP. 42: 612-617.

[9] Arunnath, A., Madhu, S. and Mebratu, T. 2022. Experimental Investigation and Optimization of Material Removal Rate and Tool Wear in the Machining of Aluminum-Boron Carbide (Al-B4C) Nanocomposite Using EDM Process. Journal of Advances in Materials Science and Engineering. Article ID 4254024.

[10] Azimi, M., Kolahdooz A. and Eftekhari, A. 2017. An Optimization on the DIN1.2080 Alloy in the Electrical Discharge Machining Process Using ANN and GA. Journal of Modern Processes in Manufacturing and Production. 6(1): 33-47.

[11] Jafari, E., Afsari A. and Abedpour, S. 2020. Predicting the Influence of Electrical Discharge Machining (EDM) Parameters on the Finished Work Surface in CK45 Steel. Journal of Modern Processes in Manufacturing and Production. 9(1): 63-78.

[12] Motevasseli, H., Afsari, A. and Khosravifard, A. 2020. Investigation of Parameters Affecting Surface Integrity and Material Removal during Electrical Discharge Machining of HARDOX-400 Steel. Journal of Modern Processes in Manufacturing and Production. 9(2): 73-84.

[13] Nguyen, H., Ngo, N. and Tuan, Q. 2020. Optimizing process parameters in EDM using low frequency vibration for material removal rate and surface roughness. Journal of King Saud University. 33(4): 284-291.

[14] Ramnath, B. 2014. Aluminium metal matrix composites–a review. Reviews on Advanced Materials Science. 38: 55-60.

[15] Data, A. 2003. NADCA product specification standards for die castings. North American Die Casting Association (NADCA), Arlington Heights, IL.

[16] Daneshmand, S., Neyestanak, A. and Monfared, V. 2008. Effects of Al2O3 powder on electro-discharge machining process of nickel-titanium shape memory alloy. Optoelectron Adv Mater Rapid Commun. 8(11-12): 1119-1124.

[17] Daneshmand, S., Kahrizi, E., LotfiNeyestanak, A. and Monfared, V. 2014. Optimization of electrical discharge machining parameters for Niti shape memory alloy by using the Taguchi method. Journal of Marine Science and Technology. 22(4): 12.